Published for SISSA by Springer

Received: May 15, 2017
Revised: August 20, 2017
Accepted: September 27, 2017
Published: October 10, 2017

Anisotropic dyonic black brane and its effects on holographic conductivity

Sunly Khimphun,[a] **Bum-Hoon Lee,**[a,b] **Chanyong Park**[b,c] **and Yun-Long Zhang**[a,b]

[a] *Center for Quantum Spacetime and Department of Physics, Sogang University, Seoul 121-742, Korea*
[b] *Asia Pacific Center for Theoretical Physics, Pohang, 790-784, Korea*
[c] *Department of Physics, POSTECH, Pohang, 790-784, Korea*

E-mail: kpslourk@sogang.ac.kr, bhl@sogang.ac.kr, chanyong.park@apctp.org, yunlong.zhang@apctp.org

Abstract: We investigate a massive gravity theory involving the SL$(2, R)$ symmetry and anisotropy. Due to the SL$(2, R)$ invariance of the equations of motion, the complex conductivity of this model transforms covariantly under the SL$(2, R)$ transformation and the ratio of DC conductivities in different spatial directions is preserved even after the SL$(2, R)$ transformation. We further investigate AC and Hall conductivities by utilizing the Kubo formula. There exists a Drude-like peak in the region with a small anisotropy, while such a Drude peak disappears when anisotropy becomes large. We also show that the complex conductivity can have a cyclotron frequency pole even beyond the hydrodynamic limit.

Keywords: Holography and condensed matter physics (AdS/CMT), AdS-CFT Correspondence, Gauge-gravity correspondence

ArXiv ePrint: 1705.00862

https://doi.org/10.1007/JHEP10(2017)064

JHEP10(2017)064

Contents

1 Introduction

Motivated from the Sting theory, the AdS/CFT correspondence has been conjectured as a duality connecting two independent theories with providing a new paradigm to understand strongly interacting conformal field theories (CFT) [1]. Recently, considerable attention has been paid to its generalization called the gauge/gravity duality in order to apply the holographic concepts to nuclear and condensed matter systems. According to the AdS/CFT correspondence, the AdS geometry can be matched with a nongravitating quantum field theory defined at the boundary of AdS. Furthermore, information about an operator of the quantum field theory is encoded into the corresponding bulk fluctuation as long as the AdS radius is sufficiently large. In this case, intriguingly, the nonperturbative properties of strongly interacting systems can be represented as classical dynamics of bulk fields in the dual asymptotic AdS space [1–4]. One of the main applications is to study the linear response in hydrodynamics, which opened a new possibility to account for transport coefficients of strongly interacting systems [5, 6]. This holographic study would be useful to understand many mysterious physical phenomena of the condensed matter theory (CMT). AdS/CMT has been intensively studied to construct a theoretical framework for figuring out unexplained properties of strongly interacting systems [7].

However, it still remains as an open problem to account for the scaling behavior of the conductivity relying on the frequency and temperature. In order to understand the unknown features of the strange metal holographically, it would be important to know the underlying structure of AdS/CMT more clearly [7]. Recently, there were attempts to explain the strange metallic behavior of cuprate with holographic models [8, 9]. As it has been known that the presence of a translational symmetry leads to an infinite DC conductivity. In order to obtain a finite conductivity, thus, one should break the translational symmetry by introducing the lattice structure or impurity. To achieve this symmetry breaking

JHEP10(2017)064

holographically, a variety of holographic models have been considered, for examples, inhomogeneous scalar field [10–13], Q-lattice [14–17] and nonlinear massive gravity [18–22]. One of the simple models reproducing a finite DC conductivity is called the linear axions model in which scalar fields linearly proportional to spatial coordinates were introduced [11]. It is related to a massive gravity theory where the momentum relaxation is described by Stüekelberg fields breaking the diffeomorphism of the gravity theory [11, 23].

In order to understand more realistic CMT phenomena, it would be important to know how the coupling constant and the linear response rely on the external field. In the Einstein-Maxwell-dilaton-axion theory which enjoy the $\mathrm{SL}(2,R)$ symmetry, it was found that a pure charged black brane solution can generate the dyonic black brane solution [24–27], which is quite helpful to study the Hall effects from holography [28, 29]. From the field theory point of view, this $\mathrm{SL}(2,R)$ transformation can be represented as the change in the coupling constant and the external electromagnetic field. In general, a condensed matter system can show totally different behaviors relying on the strength of the coupling constant. When varying the coupling constant and external electromagnetic field, the $\mathrm{SL}(2,R)$ transformation provide some clues or intuitions to understand various phases of the condensed matter systems although it is not clear whether there exists a real condensed matter system exhibiting such an $\mathrm{SL}(2,R)$ symmetry.

In CMT, another important feature is a spatial anisotropy appearing in real materials. This may be caused by the different lattice structure or the strength of the coupling constant relying on the direction, which usually breaks the rotational symmetry. In the holographic setup, such a breaking of the rational symmetry can be imitated by taking a different momentum relaxation in each spatial direction [30–36]. In the Einstein-Maxwell-dilaton-axion theory with $\mathrm{SL}(2,R)$ symmetry, the anisotropy black brane solution can also be realized by the dilaton field in [30], but the anisotropy parameter will transform under the $\mathrm{SL}(2,R)$ transformation. To avoid this inconvenience, in the present work, we include the bulk massive gravity term to break the spatial translational symmetry, as well as to induce the spatial anisotropy. The dilaton field and axion field can combine into a complex coupling field, which could be distinguished from another scalar field called Stüekelberg field of a massive gravity. A coupling between the coupling field and a gauge field whose boundary value represents an external electromagnetic field on the dual field theory side. Taking into account the linear response of the dual field theory, the change of the external field can induce a current as well as the change of the coupling constant. As a consequence, the conductivity of the present model can be represented as a function of the external field and the coupling constant. When the coupling field and vector field transform by $\mathrm{SL}(2,R)$, intriguingly, we find that a complex conductivity also transforms covariantly under the $\mathrm{SL}(2,R)$ transformation. Furthermore, we investigate the AC conductivity and its Drude behavior at low energy scale. We also discuss the cyclotron poles with comparing our results to magnetohydrodynamics (MHD) studied in [37, 38].

The rest of this paper is organized as follows. In secion 2, we consider a dyonic black hole with a spatial anisotropy and study how the $\mathrm{SL}(2,R)$ transformation is realized at the equation of motion level. On the dyonic black hole background, we investigate the conductivity of the dual theory by using the membrane paradigm in secion 3. After

JHEP10(2017)064

writing the DC conductivity in terms of the metric defined at the horizon, we study how this conductivity changes under the SL$(2,R)$ transformation. In secion 4, we study the conductivity at the asymptotic boundary by using the Kubo formula, which enables us to get more information about the linear response, for example, the AC conductivity beyond the DC conductivity. We remark our results in secion 5.

2 Massive gravity with anisotropy

It has been known that a finite DC conductivity requires the explicit breaking of the spatial translational symmetry. In the holographic model, there are several ways to break such a translational symmetry. One is to take into account scalar fields linearly proportional to spatial coordinates, which gives rise to a momentum relaxation [11, 36]. Another way is to introduce a graviton mass to break the diffeomorphism invariance. In this work, we concentrate on a massive gravity involving the SL$(2,R)$ transformation and anisotropy. Introducing additionally dilaton and axion fields to a massive gravity theory, the SL$(2,R)$ transformation can be easily realized in the massive gravity theory we consider. From now on, we call dilaton and axion fields the coupling fields for convenience. Another important feature we should note is that of the coupling field allows a coupling between electric and magnetic fields, which leads to a nontrivial Hall conductivity on the dual field theory side. In previous works on the massive gravity [18–22], a nontrivial coupling field was not considered. In this work, we will investigate how physical quantity like a conductivity is affected by the change of the coupling field and external field.

A massive gravity theory including the SL$(2,R)$ transformation and anisotropy can be described by the following action

$$S = \int d^4x\sqrt{-g}\Big[R + \frac{6}{L^2} - 2(\nabla\phi)^2 - \frac{1}{2}e^{4\phi}(\nabla\tilde{a})^2 - e^{-2\phi}F^2 - \tilde{a}F\tilde{F} \\ -p_1[\mathcal{K}] - p_2\left([\mathcal{K}]^2 - [\mathcal{K}^2]\right)\Big], \tag{2.1}$$

with dilaton field ϕ, axion field $\tilde{a}$, and electromagnetic field F. Above p_1 and p_2 are constant parameters, $[\mathcal{K}]$ indicates the trace of $\mathcal{K}^\mu{}_\nu \equiv \left(\sqrt{g^{-1}f}\right)^\mu{}_\nu$ and $[\mathcal{K}^2] = g^{\nu\mu}f_{\mu\nu}$, where $f_{\mu\nu}$ is the reference metric breaking the diffeomorphism in x- and y-directions [18–20, 39–42],

$$f_{\mu\nu} = \text{diag}\left[0, 0, k_1^2 H(z)^2, k_2^2 H(z)^2\right] . \tag{2.2}$$

Here the Stüekelberg field leads to the breaking of the diffeomorphism. For $H(z) = 1$, in addition, k_1 and k_2 correspond to the momentum relaxation. If $k_1 \neq k_2$, the graviton mass further breaks the rotational symmetry.

Einstein equations from the above action reads

$$R_{\mu\nu} - \frac{1}{2}Rg_{\mu\nu} - \frac{3}{L^2}g_{\mu\nu} = T_{\mu\nu}, \tag{2.3}$$

JHEP10(2017)064

with the energy-momentum tensor

$$T_{\mu\nu} = 2\,\nabla_\mu\phi\nabla_\nu\phi + \frac{1}{2}e^{4\phi}(\nabla_\mu\tilde{a}\nabla_\nu\tilde{a}) + 2e^{-2\phi}F_{\mu\rho}F_\nu{}^\rho - \frac{1}{2}g_{\mu\nu}\left(2(\nabla\phi)^2 + \frac{1}{2}e^{4\phi}(\nabla\tilde{a})^2 + e^{-2\phi}F^2\right)$$
$$+ \frac{1}{2}p_1\mathcal{K}_{\mu\nu} + p_2\left([\mathcal{K}]\mathcal{K}_{\mu\nu} - \left(\mathcal{K}^2\right)_{\mu\nu}\right) - \frac{1}{2}g_{\mu\nu}\left(p_1[\mathcal{K}] + p_2\left([\mathcal{K}]^2 - [\mathcal{K}^2]\right)\right). \tag{2.4}$$

After massaging this Einstein equation, all equations of motion can be summarized as

$$R_{\mu\nu} = -\frac{3}{L^2}g_{\mu\nu} + 2\nabla_\mu\phi\nabla_\nu\phi + \frac{1}{2}e^{4\phi}(\nabla_\mu\tilde{a}\nabla_\nu\tilde{a})$$
$$+ 2e^{-2\phi}F_{\mu\rho}F_\nu{}^\rho - \frac{1}{2}g_{\mu\nu}e^{-2\phi}F^2$$
$$+ \frac{1}{2}p_1\left(\mathcal{K}_{\mu\nu} + \frac{1}{2}g_{\mu\nu}[\mathcal{K}]\right) + p_2\left([\mathcal{K}]\mathcal{K}_{\mu\nu} - \left(\mathcal{K}^2\right)_{\mu\nu}\right), \tag{2.5}$$

$$\nabla_\mu\left(e^{-2\phi}F^{\mu\nu} + \tilde{a}\tilde{F}^{\mu\nu}\right) = 0\,, \tag{2.6}$$

$$\Box\phi - \frac{1}{2}e^{4\phi}(\nabla\tilde{a})^2 + \frac{1}{2}e^{-2\phi}F^2 = 0\,, \tag{2.7}$$

$$\Box\tilde{a} + 4\nabla_\mu\phi\nabla^\mu\tilde{a} - F_{\mu\nu}\tilde{F}^{\mu\nu} = 0\,. \tag{2.8}$$

Notice that there is no $\tilde{F}$ term in Einstein equation because its definition already includes $1/\sqrt{-g}$. In the case with a purely electric or magnetic field, the Chern-Simons term $F\tilde{F}$ vanishes. Due to this fact, the above equations reduce into simpler forms for a purely electric or magnetic case and it is relatively easy to solve such equations than to solve those of a general case involving nonvanishing electric and magnetic fields. First, assume that we already know a solution only for a simple case. Despite this assumption, in general, we should solve again more general equations to know a general solution. In the present model, however, we can easily know a general solution from a simple solution without solving general equations of motion. This is because the equations of the present model is invariant under the $\mathrm{SL}(2,R)$ transformation. In other words, applying the $\mathrm{SL}(2,R)$ transformation to a simple solution generates another general solution. This $\mathrm{SL}(2,R)$ transformation is very useful to understand how physical quantities of a strongly interacting system are affected by other external fields and coupling constant.

In order to see how the $\mathrm{SL}(2,R)$ transformation acts on the equations of motion, we define the coupling and vector fields as complexified forms

$$\lambda = \lambda_1 + i\lambda_2 \equiv \tilde{a}(z) + ie^{-2\phi(z)}\,, \qquad F_\pm = F \pm i\tilde{F}\,. \tag{2.9}$$

Denoting λ^* as a complex conjugate of λ, the equations of motion in (2.5)–(2.8) can be rewritten as [43]

$$R_{\mu\nu} = -\frac{3}{L^2}g_{\mu\nu} + \frac{1}{4\lambda_2^2}\left(\nabla_\mu\lambda^*\nabla_\nu\lambda + \nabla_\nu\lambda^*\nabla_\mu\lambda\right)$$
$$+ 2\lambda_2 F_{\mu\sigma}F_\nu{}^\sigma - \frac{1}{2}\lambda_2 g_{\mu\nu}F^2 + \frac{1}{2}p_1\left(\mathcal{K}_{\mu\nu} + \frac{1}{2}g_{\mu\nu}[\mathcal{K}]\right)$$
$$+ p_2\left([\mathcal{K}]\mathcal{K}_{\mu\nu} - \left(\mathcal{K}^2\right)_{\mu\nu}\right), \tag{2.10}$$

$$\nabla_\mu\left(\lambda F_+^{\mu\nu} - \lambda^* F_-^{\mu\nu}\right) = 0\,, \tag{2.11}$$

$$2\lambda_2\nabla_\mu\nabla^\mu\lambda + 2i(\nabla_\mu\lambda)(\nabla^\mu\lambda) - i\lambda_2^3 F_-^2 = 0\,, \tag{2.12}$$

JHEP10(2017)064

where $F_{\mu\sigma}F_{\nu}{}^{\sigma}$ and $F^2 = g^{\alpha\beta}F_{\alpha\sigma}F_{\beta}{}^{\sigma}$ can be reexpressed in terms of new variables

$$F_{\mu\sigma}F_{\nu}{}^{\sigma} = \frac{1}{4}\sum_{i=\pm}\sum_{j=\pm}(F_i)_{\mu\sigma}(F_j)_{\nu}{}^{\sigma}, \tag{2.13}$$

where i and j mean $+$ or $-$.

Now, let us check whether the above equations of motion are invariant under the following SL$(2,R)$ transformation

$$\begin{aligned}\lambda &\to \frac{a\lambda+b}{c\lambda+d} \qquad \text{with } ad-bc=1,\\ F_{\mu\nu} &\to (c\lambda_1+d)F_{\mu\nu} - c\lambda_2\tilde{F}_{\mu\nu}.\end{aligned} \tag{2.14}$$

To do so, we first consider the shift of λ, which is one of fundamental generators for the SL$(2,R)$ transformation. The shift, $\lambda \to \lambda + b$, is generated by the following matrix

$$\begin{pmatrix} 1 & b \\ 0 & 1 \end{pmatrix}, \tag{2.15}$$

and one can easily show that the equations of motion in (2.10)–(2.12) are invariant under this shift. Another important ingredient of the SL$(2,R)$ transformation is inversion which is generated by the following traceless unitary matrix

$$\begin{pmatrix} 0 & 1 \\ -1 & 0 \end{pmatrix}. \tag{2.16}$$

Under the inversion, the coupling fields transform as $\lambda \to \bar{\lambda} = -1/\lambda$ and $\lambda^* \to \bar{\lambda}^* = -1/\lambda^*$ and the field strengths as

$$F_+ \to -\lambda F_+\,, \qquad F_- \to -\lambda^* F_-\,. \tag{2.17}$$

When this inversion acts on the equations of motion, the equation of motion for the gauge field in (2.11) is exchanged with the Bianchi identity, whereas the equation for the coupling field in (2.12) is invariant. According to the prescriptions of ref. [24], one can also see that Einstein field equation in (2.10) is invariant under the inversion. These properties confirm that the equations of motion obtained in this model are invariant under the SL$(2,R)$ transformation. From now on, we focus on the case with $p_2 = 0$ for simplicity.

Now, let us consider a metric ansatz for a dyonic black hole with spatial anisotropy

$$ds^2 = \bar{g}_{\mu\nu}dx^\mu dx^\nu = \frac{L^2}{z^2}\left(-h(z)dt^2 + h(z)^{-1}dz^2 + e^{2U_1(z)}dx^2 + e^{2U_2(z)}dy^2\right), \tag{2.18}$$

where the unknown functions should be determined by solving equations of motion. Here, $h(z)$ indicates a black hole factor which has a root at a certain finite value of z. After an appropriate scaling, this root can be set to be 1. The existence of the root implies that the above metric represents a black hole geometry and that the black hole horizon is located at $z = 1$. Before solving equations of motion on this black hole geometry, we first think of some

JHEP10(2017)064

important features of the SL(2, R) transformation. In this model, there are two possible sources which can generate anisotropy. One is the Stüekelberg field and the other is the magnetic field strength. If we introduce a constant magnetic field strength, the anisotropy of this model is governed by only the Stüekelberg field. In this case, the anisotropy of the metric ansatz is directly related to that of Stüekelberg field. More precisely, since isotropy is restored for $k_1 = k_2$, $U_1(z)$ and $U_2(z)$ could be reduced to the same function in that case. This implies that the anisotropy of the metric ansatz is determined in terms of the Stüekelberg field

$$e^{U_1(z)-U_2(z)} = F\left(\frac{k_1}{k_2}\right), \tag{2.19}$$

where the function F satisfy $F(1) = 1$ in order to obtain the isotropic case correctly. From the definition of $\mathcal{K}$ ($\mathcal{K}^\mu{}_\sigma \mathcal{K}^\sigma{}_\nu \equiv g^{\mu\sigma} f_{\sigma\nu}$), we can absorb the anisotropy of the Stüekelberg field into the metric. Then, the resulting Stüekelberg field becomes symmetric, so the metric absorbing the anisotropy of the Stüekelberg field could also be isotropic, if k_1 and k_2 are non-zero parameters. This fact requires the following relation

$$e^{-2U_1(z)}k_1^2 = e^{-2U_2(z)}k_2^2. \tag{2.20}$$

This relation determines the anisotropy of the metric in terms of that of the Stüekelberg field

$$\frac{e^{U_1(z)}}{e^{U_2(z)}} = \frac{k_1}{k_2}\,. \tag{2.21}$$

This corresponding to a special class with a constant magnetic field strength. In the section 4, we will show that there exists another type of numerical solution with a magnetic field strength varying in the radial direction which allows a solution with an isotropy at the boundary but with an anisotropic space at the horizon.

The SL(2, R) transformation is useful to generate a new solution from a known solution without solving equations of motion, because of the invariance of equations of motion under the SL(2, R) transformation. To see this, let us first consider a purely electrically charged solution, whose gauge field has only the time component

$$A_\mu dx^\mu = A_t(z)dt\,. \tag{2.22}$$

Using the above metric ansatz, one can easily find a conserved electric charge, $Q = -e^{U_1+U_2-2\phi}A_t'$, and then the electric field can be rewritten in terms of this conserved electric charge

$$F = e^{-U_1-U_2}(\lambda_2)^{-1}Q\,dt\wedge dz\,. \tag{2.23}$$

In a more general situation with nonvanishing electric and magnetic fields, the corresponding field strengths are given by [28]

$$\bar{F} = (\bar{\lambda}_2)^{-1}e^{-U_1-U_2}\left(\bar{Q}_e - \bar{\lambda}_1\bar{Q}_m\right)\,dt\wedge dz + \bar{Q}_m dx\wedge dy\,, \tag{2.24}$$

where the bar indicates the quantities obtained in the general case with nontrivial electric and magnetic fields. In the present model, the above two electromagnetic fields derived from different situations can be connected to each other by the SL(2, R) transformation.

JHEP10(2017)064

After some calculation, it shows that the electromagnetic charges are related by the SL$(2,R)$ parameters $\bar{Q}_e = a\,Q$ and $\bar{Q}_m = c\,Q$. From another viewpoint, if we know the electromagnetic charges and the coupling constants of two different solutions, the SL$(2,R)$ parameters can be fixed by these quantities. In the above case,

$$\begin{aligned} a &= \bar{Q}_e/Q\,, \\ c &= \bar{Q}_m/Q\,. \end{aligned} \tag{2.25}$$

The remaining SL$(2,R)$ parameters can also be determined by regarding the transformation of the coupling constants. For example, we can take the value of coupling fields either at either boundary $z = 0$ or horizon $z = 1$, the SL$(2,R)$ transformation gives rise to the following relation [28]

$$d = \frac{Q\left(\bar{Q}_e - \bar{Q}_m\bar{\lambda}_1\right)}{\left(\bar{Q}_e - \bar{\lambda}_1\bar{Q}_m\right)^2 + \left(\bar{Q}_m\bar{\lambda}_2\right)^2}\Big|_{z\to 0}\,, \tag{2.26}$$

From the constraint of the SL$(2,R)$ transformation, $ad - bc = 1$, we finally obtain

$$b = \frac{Q\left(\bar{Q}_e\bar{\lambda}_1 - \bar{Q}_m\left(\bar{\lambda}_1^2 + \bar{\lambda}_2^2\right)\right)}{\left(\bar{Q}_e - \bar{\lambda}_1\bar{Q}_m\right)^2 + \left(\bar{Q}_m\bar{\lambda}_2\right)^2}\Big|_{z\to 0}\,. \tag{2.27}$$

Since a and c are determined in terms of background electromagnetic charges in (2.25), solving the above relations in (2.26) and (2.27) can uniquely determines the remaining parameters, b and d.

For the purely electric case the axion is decoupled from the vector field, so hereafter we set $\lambda_1 = 0$ for the purely electric case. Even in this case, the SL$(2,R)$ transformation (2.14) generates a nonvanishing axion and dilaton fields

$$\bar{\lambda}_1 = \frac{ac\lambda_2^2 + bd}{c^2\lambda_2^2 + d^2}, \qquad \bar{\lambda}_2 = \frac{\lambda_2}{c^2\lambda_2^2 + d^2}\,. \tag{2.28}$$

The most general cases can be obtained by applying the SL$(2,R)$ transformation successively. As shown in this example, the SL$(2,R)$ symmetry plays an important role in generating a new general solution. The transformed coupling fields, $\bar{\lambda}_1$ and $\bar{\lambda}_2$, are again represented in terms of SL$(2,R)$ parameters and the coupling field λ_2 of the purely electric case. In the next section, we will further investigate how the SL$(2,R)$ transformation modifies the physical quantities like the conductivity.

3 Holographic DC and hall conductivities

In the holographic studies, there exist two methods to derive the conductivity of the dual field theory. One is known as the membrane paradigm [44, 45] and the other uses the Kubo formula [5, 6]. In the membrane paradigm, the DC conductivity is determined in terms of the background metric at the black hole horizon. The membrane paradigm is a useful method to investigate the DC conductivity because it enables us to write down its analytic form exactly. When we investigate the AC conductivity, unfortunately, the membrane paradigm is not helpful because it contains only information about the $\omega = 0$

JHEP10(2017)064

limit. In order to study the AC conductivity, we can utilize the Kubo formula, instead of the membrane paradigm, near the asymptotic boundary. Although it does not allow us to write down the analytic form of AC conductivity in terms of the background metric, the Kubo formula is useful to obtain the numerical values of the AC as well as DC conductivities. In this case, the DC conductivity is obtained by taking the $\omega = 0$ limit of the AC conductivity and the Kubo formula leads to the same result derived from the membrane paradigm [45–51]. In this section, we will investigate how the SL$(2, R)$ transformation changes the DC conductivity analytically. To do so, we will apply the membrane paradigm technique. Based on the results obtained in this section, in the next section 4 we will further investigate the AC conductivity numerically by using the Kubo formula.

3.1 DC and hall conductivities with electric and magnetic fields

In the previous section 2, we studied how the black hole solutions transform under the SL$(2, R)$ transformation. In this section, we will investigate how such changes modify physical quantities by using the membrane paradigm. In order to study the DC conductivity on the general dyonic black hole geometry, we take account of the following background gauge field

$$\bar{A} = \bar{A}_t(z)dt + \bar{A}_y(x)dy, \tag{3.1}$$

where we denote the background fields with the bar symbol. In this case, the equation of $\bar{A}_y(x)$ is simply reduced to $\partial^x\partial_x\bar{A}_y(x) = 0$, so we can take $\bar{A}_y(x) = \bar{Q}_m x$ where $\bar{Q}_m$ corresponds to the magnetic field. Comparing it with (2.24), moreover, it is equal to the magnetic charge of the dyonic black hole.

In order to obtain the general DC conductivity involving the effects of the axion, dilaton, and Chern-Simons term, let us first consider the relatively simple case with $\lambda_1(1) = 0$ at the horizon and $\bar{Q}_m \neq 0$. This case can be easily achieved by applying the SL$(2, R)$ transformation to the purely electrically charged case. For example, we can take the SL$(2, R)$ parameters in (2.28) to be $ac\lambda_2^2 + bd = 0$ at the horizon. This condition removes the axion and Chern-Simons term at least at the horizon and enables us to calculate the DC conductivity more easily. If we further set $\phi = 0$, or say, $\lambda_2 = 1$, our model becomes similar to the previous works up to anisotropy [52–56]. Applying the SL$(2, R)$ transformation successively, then we can obtain a more general result with nonvanishing axion and Chern-Simons term (see the next subsection).

Turning on vector fluctuations of the metric and gauge field

$$\delta A_i dx^i = (A_x(z) - E_x t)\, dx + (A_y(z) - E_y t)\, dy\,, \tag{3.2}$$

$$\delta g_{\mu\nu}dx^\mu dx^\nu = \frac{2L^2}{z^2}\left(\delta g_{ti}(z)\, dtdx^i + \delta g_{zi}(z)\, dzdx^i\right)\,, \tag{3.3}$$

where i, j means 1 or 2 with $\{x^1, x^2\} = \{x, y\}$. Moreover, the ti-component yields Noting that A_i behaves as $A_i = -E_i/h + \mathcal{O}(1 - z)$ near the horizon. Also, by using regularity of Eddington-Finkelstein coordinate so that $\delta g_{ti} \sim h\, \delta g_{zi}|_{z\to 1}$, we obtain asymptotic

JHEP10(2017)064

expression as [52–55]

$$\delta g_{ti}=-\frac{4e^{2U_j}\left[\epsilon_{ij}\bar{Q}_m E_j\left(4\bar{Q}_m^2+\tilde{p}_1 k_j e^{U_s+U_i}\bar{\lambda}_2^{-1}+4e^{2U_s}A_t'^2\right)+\tilde{p}_1 k_j e^{2U_s+U_j}\bar{\lambda}_2^{-1}E_i A_t'\right]}{16\bar{Q}_m^4+4\bar{Q}_m^2 e^{U_s}\bar{\lambda}_2^{-1}\tilde{p}_1\left(e^{U_j}k_i+e^{U_i}k_j\right)+e^{2U_s}\left(\bar{\lambda}_2^{-2}e^{U_s}\tilde{p}_1^2 k_i k_j+16\bar{Q}_m^2 A_t'^2\right)}\,, \tag{3.4}$$

where $\epsilon_{xy}=-\epsilon_{yx}=1$ and A_t' is given in (2.24). For the equations in this paper, we make the conversion that the lower indexes will not be summed. When $i=x$, we set $j=y$, and vice verse. We combined U_1 and U_2 into symmetric and antisymmetric notations, $U_s=U_1+U_2$ and $U_a=U_1-U_2$, and introduced $\tilde{p}_1=p_1 H(z)$ for convenience.

Varying the quadratic action with the vector fluctuations, the corresponding conserved currents are given by

$$J_i=-he^{-\epsilon_{ij}U_a}\bar{\lambda}_2 A_i'+e^{-2U_i}\bar{Q}_m\delta g_{ti}-he^{-U_s}\bar{Q}_m\bar{\lambda}_2\delta g_{zj}-\left(E_j+\bar{Q}_m e^{-2U_i}\delta g_{ti}\right)\bar{\lambda}_1\,, \tag{3.5}$$

After substituting the fluctuation solutions into the current relations and comparing it with the Ohm's law

$$\begin{pmatrix}J_x\\J_y\end{pmatrix}=\begin{pmatrix}\sigma_{xx}&\sigma_{xy}\\\sigma_{yx}&\sigma_{yy}\end{pmatrix}\begin{pmatrix}F_{tx}\\F_{ty}\end{pmatrix}\,, \tag{3.6}$$

the membrane paradigm defined at the horizon leads to the following DC conductivity

$$\bar{\sigma}_{ii}=\frac{N_{ii}}{D}\,,\qquad \bar{\sigma}_{xy}=-\bar{\sigma}_{yx}=\frac{N_{xy}}{D}\,, \tag{3.7}$$

where

$$\begin{aligned}
N_{ii}&=\tilde{p}_1 k_j e^{U_s+U_j}\left[\tilde{p}_1 k_i\bar{\lambda}_2^{-1}e^{U_s+U_j}+4\bar{Q}_m^2\left(1+\bar{\lambda}_1^2\bar{\lambda}_2^{-2}\right)+4\bar{\lambda}_2^{-2}\bar{Q}_e\left(\bar{Q}_e-2\bar{Q}_m\bar{\lambda}_1\right)\right]\\
N_{xy}&=4\bar{Q}_m\bar{Q}_e\left[\tilde{p}_1\bar{\lambda}_2^{-1}e^{U_s}\left(k_1e^{U_2}+k_2e^{U_1}\right)+4\bar{Q}_e^2\bar{\lambda}_2^{-2}\right]+\left(\tilde{p}_1^2k_1k_2e^{3U_s}-32(\bar{Q}_e\bar{Q}_m)^2\right)\bar{\lambda}_2^{-2}\bar{\lambda}_1\\
&\quad+16\bar{Q}_e\bar{Q}_m^3\left(1+\bar{\lambda}_1^2\bar{\lambda}_2^{-2}\right)\\
D&=\bar{\lambda}_2^{-1}\left[4\bar{Q}_m^2\left(4\bar{\lambda}_2^{-1}\bar{Q}_e^2+\tilde{p}_1e^{U_s}\left(k_1e^{U_2}+k_2e^{U_1}\right)\right)+\left(\tilde{p}_1^2k_1k_2e^{3U_s}-32\bar{Q}_e\bar{Q}_m^3\bar{\lambda}_1\right)\right]\\
&\quad+16\bar{Q}_m^4\left(1+\bar{\lambda}_1^2\bar{\lambda}_2^{-2}\right)
\end{aligned}$$

The above conductivities have several remarkable peoperties. Under $x\leftrightarrow y$, $k_1\leftrightarrow k_2$ and $U_1\leftrightarrow U_2$, σ_{xy} is invariant and σ_{xx} and σ_{yy} are exchanged into each other. When $k_1=k_2$, furthermore, $U_1=U_2$ and $\sigma_{xx}=\sigma_{yy}$, so the rotational symmetry is restored as expected. This is consistent with our previous metric ansatz. When $k_1=k_2$, this result exactly reduces the one obtained in ref. [12]. If we use the special solution in (2.21), we can see that the ratio of $\bar{\sigma}_{yy}$ and $\bar{\sigma}_{xx}$ relies only on the spatial components of the metric

$$\frac{\bar{\sigma}_{yy}}{\bar{\sigma}_{xx}}=e^{2U_a(1)}. \tag{3.8}$$

This further implies that the ratio of DC conductivities in different spatial directions is equal to the square of anisotropy

$$\frac{\bar{\sigma}_{yy}}{\bar{\sigma}_{xx}}=\left(\frac{k_1}{k_2}\right)^2. \tag{3.9}$$

Lastly, when the magnetic charge of the background black hole is absent, the Hall conductivity disappears as expected. In this model, because of anisotropy, the Hall angles in different directions, $\cot\theta_x\equiv\bar{\sigma}_{xx}/\bar{\sigma}_{xy}$ and $\cot\theta_y\equiv\bar{\sigma}_{yy}/\bar{\sigma}_{xy}$, show different behaviors. However, they satisfy the following relation, $k_2^2\cot\theta_y=k_1^2\cot\theta_x$.

JHEP10(2017)064

3.2 SL(2, R) transformation of a complex conductivity

In the previous section, we calculated DC and Hall conductivities by using the membrane paradigm. In addition, we also found a new relation between DC conductivities, $\bar{\sigma}_{yy} = e^{2U_a}\bar{\sigma}_{xx}$. From the result obtained in the previous section, in this section, we explain how we can obtain more general conductivities with the nonvanishing axion field $\bar{\lambda}_1$ at the horizon by applying the SL(2, R) transformation. To do so, let us first introduce a complex conductivity as the combination

$$\sigma_\pm \equiv \sigma_1 \pm iG\sigma_2\,, \tag{3.10}$$

where $\sigma_1 = \sigma_{yx}/4$ and $\sigma_2 = \sigma_{xx}/4$ and $G = e^{U_a}$. Then, we can see that this complex conductivity transforms covariantly under the SL(2, R) transformation

$$\sigma_\pm \to \frac{a\sigma_\pm + b}{c\sigma_\pm + d}\,. \tag{3.11}$$

In order to check this statement, let us recall that the dual currents can be represented as the following forms

$$J_x = 4\left(\sigma_2 F_{tx} - \sigma_1 F_{ty}\right) = 4\left(\lambda_2 F_{zx} - \lambda_1 F_{ty}\right), \tag{3.12}$$

$$J_y = 4\left(\sigma_1 F_{tx} + G^2\sigma_2 F_{ty}\right) = 4\left(\lambda_2 F_{zy} + \lambda_1 F_{tx}\right). \tag{3.13}$$

In each line, the terms after the first equal sign are nothing but the definition of the linear response theory, while the terms after the second equal sign indicate the Noether currents of vector fluctuations. These equalities are generally satisfied if we consider the bulk fluctuations in (3.2), and it can be evaluated at both of the horizon $z = 1$ and the boundary $z = 0$. We will see that the above relations have to be satisfied even after the SL(2, R) transformation.

First, assuming the SL(2, R) transformation of $\sigma_\pm$ in (3.11), we can easily see that the shift of λ and $\sigma_\pm$, $\lambda \to \lambda + b$ and $\sigma_\pm + b$, does not break the equalities in (3.12) and (3.13). Another transformation we should consider to confirm the SL(2, R) transformation is the inversion. After the inversion, the last terms of (3.12) and (3.13) reduce to $-F_{ty}$ and F_{tx} respectively. Under the assumption in (3.11), we can also see that the definitions of the linear response in (3.12) and (3.13) reduce to the same values, $-F_{ty}$ and F_{tx}. As a consequence, the relations in (3.12) and (3.13) are still satisfied under the covariant SL(2, R) transformation of $\sigma_\pm$, as it should do.

As mentioned before, the SL(2, R) transformation is important to generate a general solution involving nonvanishing electromagnetic charges and a nontrivial coupling constant. Similarly, the covariant SL(2, R) transformation of $\sigma_\pm$ is useful to know the conductivities of such a complicated system. When turning on the axion field and Chern-Simons terms, the resulting equations for fluctuations becomes more complicated because of the nontrivial coupling with the axion field. In this case, we can easily obtain the conductivity by applying the SL(2, R) transformation instead of solving the complicated equations. Starting the case with $\lambda_1(1) = 0$ and apply the SL(2, R) transformation, we can find the more general

JHEP10(2017)064

conductivities

$$\begin{aligned}\bar{\sigma}_{xx} &= \frac{16\sigma_{xx}}{c^2\sigma_{xx}\sigma_{yy}+(c\sigma_{xy}-4d)^2}\,,\\ \bar{\sigma}_{xy}=-\bar{\sigma}_{yx} &= -\frac{4ac\sigma_{xx}\sigma_{yy}+4\,(a\sigma_{xy}-4b)\,(c\sigma_{xy}-4d)}{c^2\sigma_{xx}\sigma_{yy}+(c\sigma_{xy}-4d)^2}\,,\\ \bar{\sigma}_{yy} &= \frac{16\sigma_{yy}}{c^2\sigma_{xx}\sigma_{yy}+(c\sigma_{xy}-4d)^2}\,,\end{aligned} \tag{3.14}$$

where σ_{ij} indicates the given conductivity and $\bar{\sigma}_{ij}$ denotes the conductivity after the SL$(2,R)$ transformation. In particular, from the initial case with $\lambda_1 = 0$, we can obtain the nonvanishing axion and dilaton fields at the horizion

$$\bar{\lambda}_1(1) = \frac{ac\lambda_2^2+bd}{c^2\lambda_2^2+d^2}\Big|_{z=1} \quad \text{and} \quad \bar{\lambda}_2(1) = \frac{\lambda_2}{c^2\lambda_2^2+d^2}\Big|_{z=1}. \tag{3.15}$$

As shown in this simple example, the SL$(2,R)$ transformation is useful to obtain the conductivity for the general case with a nonvanishing axion field and Chern-Simons term. For example, if taking $a = d = 1, c = 0$ in (3.14) and (3.15), we have $\bar{\sigma}_{xy} = \sigma_{xy} - 4\bar{\lambda}_1|_{z=1} = \sigma_{xy} - 4\tilde{a}|_{z=1}$, that the term linear in $\tilde{a}$ appear in the Hall conductivity, which matches with the result in [55]. Furthermore, we found that the ratio of DC conductivities, $\sigma_{yy}/\sigma_{xx} = G^2$, is preserved even under the SL$(2,R)$ transformation.

4 AC conductivity from the Kubo formula

In this section, we will study the holographic conductivity by using the Kubo formula. Although the DC and Hall conductivities were studied in the previous section by using the membrane paradigm, the Kubo formula is useful to get more information about the AC conductivity. First, we briefly describe how one can obtain DC and AC conductivities by using the Kubo formula and compare the resulting DC conductivity with that obtained by the membrane paradigm for a purely electrically charged case. And then we discuss the AC conductivity in more general cases with non-vanishing electromagnetic charges. Using the metric ansatz in (2.18) and gauge field in (2.23), the equations of motion in (2.5)–(2.8) reduce to

$$\phi'^2 + \frac{1}{4}e^{4\phi}\tilde{a}'^2 + \frac{U_s'^2}{4} + \frac{U_a'^2}{4} + \frac{U_s''}{2} = 0\,, \tag{4.1}$$

$$\frac{1}{4}\tilde{p}_1 e^{-U_s/2}\left(k_2 e^{U_a/2} - k_1 e^{-U_a/2}\right) + \left[h\left(zU_s' - 2\right) + zh'\right]\frac{U_a'}{2} + \frac{hzU_a''}{2} = 0\,, \tag{4.2}$$

$$\begin{aligned}&2z\tilde{p}_1 e^{-U_s/2}\left(k_1 e^{-U_a/2} + k_2 e^{U_a/2}\right) - 4z^4Q^2e^{2\phi-2U_s} + 12\\ &+\left(8zU_s' - z^2U_s'^2 + z^2U_a'^2 + 4z^2\phi'^2 + z^2e^{4\phi}\tilde{a}'^2 - 12\right)h + 2z\left(2 - zU_s'\right)h' = 0\,,\end{aligned} \tag{4.3}$$

$$Q^2z^3e^{2\phi-2U_s} - \frac{1}{2}hze^{4\phi}\tilde{a}'^2 + \left(hzU_s' + zh' - 2h\right)\phi' + hz\phi\text{“} = 0\,, \tag{4.4}$$

$$\left[h\left(zU_s' + 4z\phi' - 2\right) + zh'\right]\tilde{a}' + hz\tilde{a}'' = 0\,. \tag{4.5}$$

JHEP10(2017)064

If $H(z)$ is a constant, the massive gravity theory with anisotropy becomes similar to another momentum relaxation model represented by linear scalar fields [36]. In the present work, thus, we consider a more general case with $H(z) = z$.

Note that equations of motion in (4.1)–(4.5) are invariant under the shift of scalar fields

$$\phi \to \phi - \phi_0\,, \qquad Q \to e^{\phi_0} Q\,, \qquad \tilde{a} \to e^{2\phi_0}\tilde{a}, \tag{4.6}$$

and under the scaling of coordinates x, y and parameters k_1, k_2,

$$\begin{aligned} x &\to e^{-(U_s(0)+U_a(0))/2} x\,, & k_1 &\to e^{-(U_s(0)+U_a(0))/2} k_1\,, \\ y &\to e^{-(U_s(0)-U_a(0))/2} y\,, & k_2 &\to e^{-(U_s(0)-U_a(0))/2} k_2\,, \end{aligned} \tag{4.7}$$

where $U_s(0)$ and $U_a(0)$ indicate the boundary values of spatial metric components at $z = 0$. The existence of the horizon requires $h(z)$ to be $h(1) = 0$ where the horizon is located at $z = 1$. Due to the above scaling invariances, some variables at the horizon are determined in terms of intrinsic parameters

$$\begin{aligned} \phi'(1) &= \frac{2(k_1 + k_2 + 2k_1k_2) + Q^2}{\kappa}\,, & \tilde{a}'(1) &= 0, \\ U_s'(1) &= \frac{2(\kappa + Q^2) - (6 + k_1 + k_2 + k_1k_2)}{\kappa}\,, & U_a'(1) &= \frac{k_2 - k_1}{2\kappa}, \end{aligned} \tag{4.8}$$

where $\kappa = -h'(1)$ is associated with the Hawking temperature via $\kappa = 4\pi T$. When we solve equations of motion numerically, these relations play a role of boundary conditions at the horizon. In figure 1, we depict numerical solutions satisfying the above boundary conditions and equations of motion. In the case with only an electric charge, a constant axion field becomes the solution of (2.8) because the absence of the magnetic field, and we simply choose $\tilde{a} = 0$ for the pure electronic case.

In order to obtain DC and AC conductivities by using the Kubo formula, we turn on vector and metric fluctuations on the above background numerical solution

$$\begin{aligned} A &= \bar{A}_t(z)dt + \left(\tilde{A}_x(t,z)dx + \tilde{A}_y(t,z)dy\right)\,, \\ ds^2 &= \bar{g}_{\mu\nu}dx^\mu dx^\nu + \frac{2L^2}{z^2}\left(\tilde{g}_{ti}(t,z)dtdx^i + \tilde{g}_{zi}(t,z)dzdx^i\right)\,, \end{aligned}$$

where $\bar{A}_t$ and $\bar{g}_{ab}$ indicate the background solutions in (2.18) (2.22), and the tilde symbol was used to denote their fluctuations. We will use the Fourier mode expansion

$$\begin{aligned} \tilde{A}_i(t,z) &= \int_{-\infty}^{\infty}\frac{d\omega}{2\pi}e^{-i\omega t}A_i(z), & \tilde{g}_{ti}(t,z) &= \int_{-\infty}^{\infty}\frac{d\omega}{2\pi}e^{-i\omega t}g_{ti}(z)\,, \\ \tilde{g}_{zi}(t,z) &= \int_{-\infty}^{\infty}\frac{d\omega}{2\pi}i\omega e^{-i\omega t}g_{zi}(z)\,. \end{aligned}$$

JHEP10(2017)064

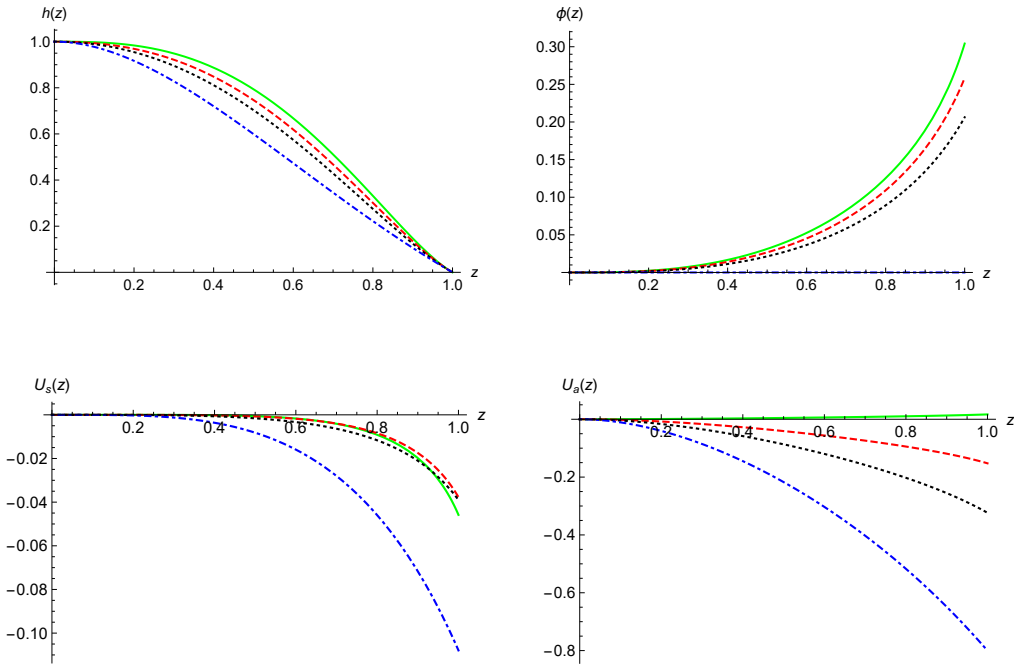

Figure 1. Plots of the functions in the metric and dilaton fields in terms of coordinate z , for fixed $p_1 = 1$, $k_1 = 0.1$, $\kappa = 1$, with $k_2 = 0$ (Green), 1 (Red-dashed), 2 (Black-dotted), and 4.8294 (Blue-dotted-dashed).

Considering the equations of motion (2.5)–(2.8), as well as (4.1)–(4.5) for the background, the fluctuation equations are reduced to

$$0 = \left(\frac{-k_i p_1 Q H e^{-3U_s/2-\epsilon_{ij}U_a/2+2\phi}}{z}\right) g_{zi} + \left(\frac{\omega^2}{h^2} - \frac{4Q^2 z^2 e^{-2U_s+2\phi}}{h}\right) A_i + \left(-\epsilon_{ij}U_a' + \frac{h'}{h} - 2\phi'\right) A_i' + A_i'' \,, \tag{4.9}$$

$$0 = -4Q z^2 e^{-U_s} A_i - \left(\omega^2 - \frac{k_i p_1 H h e^{-U_s/2-\epsilon_{ij}U_a/2}}{z}\right) g_{zi} + \left(-U_s' - \epsilon_{ij}U_a\right) g_{ti} + g_{ti}' \,, \tag{4.10}$$

$$0 = \frac{g_{ti}}{h^2} + \left(\frac{H'}{H} - \frac{3}{z} + \frac{h'}{h} + \frac{U_s}{2} - \epsilon_{ij}\frac{U_a}{2}\right) g_{zi} + g_{zi}' \,, \tag{4.11}$$

To solve these equations, let us first investigate solutions near the horizon. (4.9)–(4.11) are singular at the horizon because $h(1) = 0$. In order to satisfy equations, fluctuations must have appropriate singularity at the horizon. Introducing new variables with an appropriate exponent γ,

$$\hat{A}_i(z) \equiv h(z) A_i'(z) \,, \tag{4.12}$$

and

$$A_i(z) = (1-z)^\gamma a_i(z) \,, \qquad \hat{A}_i(z) = (1-z)^\gamma \hat{a}_i(z) \,,$$
$$g_{ti}(z) = (1-z)^\gamma \zeta_{ti}(z) \,, \qquad g_{zi}(z) = (1-z)^\gamma \zeta_{zi}(z)/h(z). \tag{4.13}$$

JHEP10(2017)064

the above equations reduce to four first-order differential equations near the horizon

$$
\begin{aligned}
0 &= \hat{a}_i' - \left(\epsilon_{ij}U_a' + \frac{\gamma}{1-z} + 2\phi'\right)\hat{a}_i + \left(\frac{\omega^2}{h} - 4z^2 e^{2\phi - 2U_s}Q^2\right)a_i \\
&\quad + \frac{1}{z}p_1 k_i H e^{2\phi - 3U_s/2 - \epsilon_{ij}U_a/2}\zeta_{zi}\,, \\
0 &= a_i' - \frac{\gamma}{1-z}a_i - \frac{\hat{a}_i}{h}\,, \\
0 &= \zeta_{zi}' + \left(\frac{H'}{H} + \frac{U_s'}{2} - \epsilon_{ij}\frac{U_a'}{2} - \frac{\gamma}{1-z} - \frac{3}{z}\right)\zeta_{ti} + \frac{\zeta_{ti}}{h}\,, \\
0 &= \zeta_{ti}' - \left(\left(U_s' + \epsilon_{ij}U_a'\right) + \frac{\gamma}{1-z}\right)\zeta_{ti} - \left(\frac{\omega^2}{h} - \frac{1}{z}p_1 k_i H e^{-(U_s/2 + \epsilon_{ij}U_a/2)}\right)\zeta_{zi} \\
&\quad - 4z^2 Q e^{-U_s}a_i.
\end{aligned}
\tag{4.14}
$$

Rewriting these equations as the eigenvalue equation form, we obtain

$$
\begin{pmatrix}
0 & -\frac{\omega^2}{h'(1)} & 0 & 0 \\
\frac{1}{h'(1)} & 0 & 0 & 0 \\
0 & 0 & 0 & -\frac{1}{h'(1)} \\
0 & 0 & \frac{\omega^2}{h'(1)} & 0
\end{pmatrix}
\begin{pmatrix} \hat{a}_i \\ a_i \\ \zeta_{zi} \\ \zeta_{ti} \end{pmatrix}
= \gamma
\begin{pmatrix} \hat{a}_i \\ a_i \\ \zeta_{zi} \\ \zeta_{ti} \end{pmatrix}.
\tag{4.15}
$$

This eigenenvalue equation allows degenerated eigenvalues, $\gamma = \pm\frac{i\omega}{h'(1)}$, and their eigenvectors are given by [36, 57]

$$
\psi_{1\pm} = \begin{pmatrix} 0 \\ 0 \\ \pm i/\omega \\ 1 \end{pmatrix}, \quad \psi_{2\pm} = \begin{pmatrix} \pm i\omega \\ 1 \\ 0 \\ 0 \end{pmatrix}.
\tag{4.16}
$$

Here, two eigenvectors, ψ_{1-} and ψ_{2-} correspond to incoming solutions, whereas the others describe outgoing solutions.

After picking the incoming solutions up, solving equations in (4.9)–(4.11) numerically gives rise to information about boundary behaviors of fluctuations. Then, the Kubo formula together with these numerical solutions determines numerical values of DC and AC conductivities (see [13, 16, 17, 36] for more details). In figure 2, we plot DC conductivity obtained by the Kubo formula, which is well matched to the result obtained from the membrane paradigm, as expected.

Unlike the membrane paradigm used in the previous section, the Kubo formula allows us to get more information on the AC conductivity. Repeating the same calculation with a nonvanishing frequency, we know at least numerically how the AC conductivity relies on the frequency. For $\bar{Q}_m = 0$, in figure 3, we plot the real and imaginary parts of the AC conductivity and the scaling behaviors in the low frequency regime with several different values of k_2. In the left hand side plots of figure 3, the AC conductivities in the low frequency regime show a Drude-like behavior for small k_2. In this case, the small k_2 indicates a small anisotropy because we take $k_1 = 0.1$. The numerical result shows that the

JHEP10(2017)064

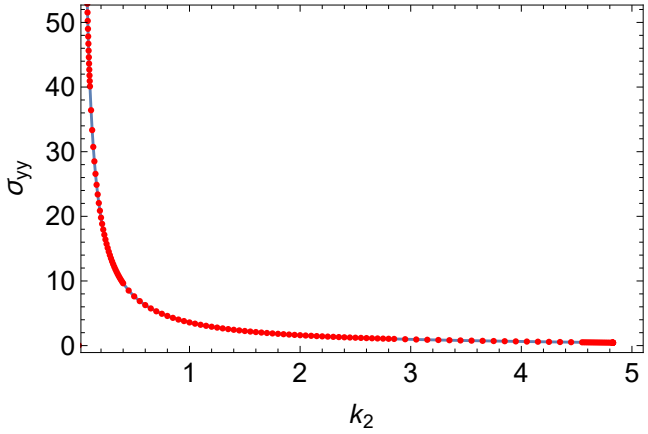

Figure 2. The DC conductivity σ_{yy} in terms of parameter k_2, for fixed $p_1 = 1$, and $k_1 = 0.1$. The red dots are from Kubo formula, and they match to the result(blue curve) obtained from the membrane paradigm in (3.7).

Drude-like peak becomes flattened as anisotropy increases and then at a certain critical value the peak disappears. This becomes manifest in the left hand side of the bottom figure in figure 3 because there is no Drude-like peak for a large anisotropy (or large k_2). We further find that the Drude-like peak disappears near $k_2 \approx 4.82$ for $k_1 = 0.1$. The similar behaviors in both normal and superconducting phases have also been observed at low temperature [58–60]. In the right hand side figures of figure 3, we present the power-law scaling behavior of the AC conductivity

$$|\sigma_{yy}| \sim \omega^{-\alpha}. \tag{4.17}$$

The result shows that there exists such a power-law scaling behavior and that the scaling exponent α becomes smaller as the anisotropy increases. At a certain critical value, furthermore, it becomes zero and then changes the sign. This qualitative behavior is consistent with the disappearance of the Drude-like peak mentioned before. It has been known that the normal mode of cuprates and high-T_c superconductor shows a universal scaling behaviors of the optical conductivity with $\alpha = 2/3$ [61]. So it would be interesting to see how the anisotropy affects such a universal scaling behavior in the future work.

Now, let us take into account more general situations having a nonvanishing magnetic field as in (2.24). After adding a background magnetic field denoted by $\bar{Q}_m$ and repeating the previous calculations done without $\bar{Q}_m$, we can get numerical information about conductivities of the dual field theory. On the other hand, the SL$(2, R)$ transformation of the conductivities in (3.14) can also be applied to the AC conductivities, with the parameters being fixed from (2.25)–(2.27). In this case, due to the nonvanishing magnetic field, we could generate the Hall conductivity as well as AC conductivity from the pure electric case in figure 3.

In figure 4, we add the plots $\bar{\lambda}_1(z)$ and $\bar{\lambda}_2(z)$ for different values of $\bar{Q}_m$ and $\bar{Q}_e$, along with $k_1 = 0.1$, $k_2 = 0.4$. We have choosen the boundary condition $\bar{\lambda}_2(0) = 1$, such that the

JHEP10(2017)064

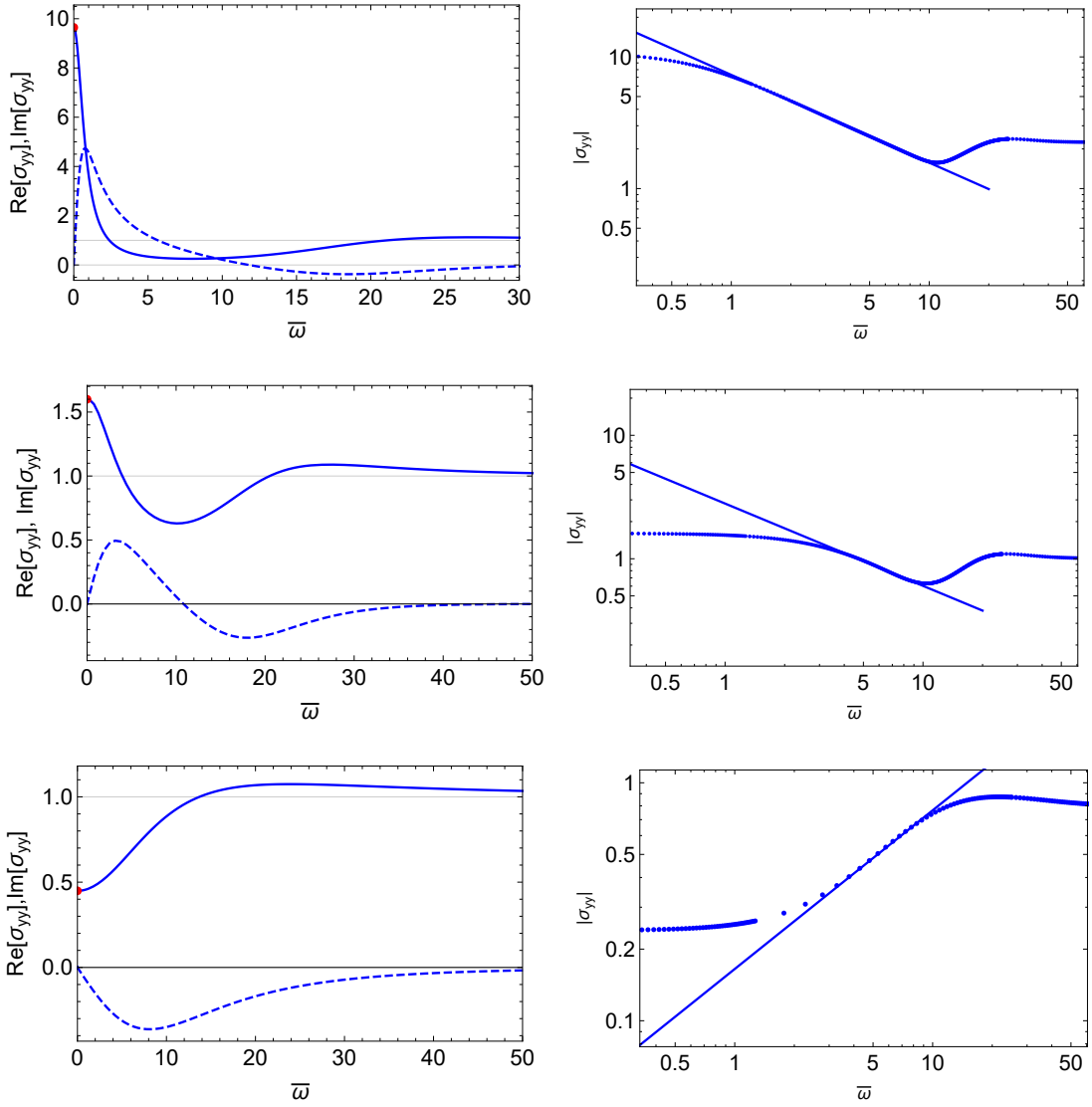

Figure 3. Left column: the real (solid) and imaginary (dashed) parts of the AC conductivities σ_{yy} in terms of frequency ω, for $k_2 = 0.4$ (top), 2 (middle) and 4.8295 (bottom), where we take $p_1 = 1$ and $k_1 = 0.1$ and used $\bar{\omega} = \omega/T$. Right column: the Log-Log plots for $|\sigma_{yy}| \sim \bar{\omega}^{-\alpha}$, where $|\sigma_{yy}| = \sqrt{\mathrm{Re}[\sigma_{yy}]^2 + \mathrm{Im}[\sigma_{yy}]^2}$, and from top to down, $\alpha \simeq 2/3, 2/3, -2/3$, respectively.

parameters in the SL(2,R) transformation can be fixed via (2.25)–(2.27). Then $\bar{\lambda}_1(z)$ and $\bar{\lambda}_2(z)$ could be transformed by these parameters through (2.28).

In figure 5, we depict various AC and Hall conductivities relying on the frequency with different values of $\bar{Q}_m$ and fixed $\bar{Q}_e$. The result shows that the peaks of AC and Hall conductivities move to the high frequency regime as the strength of the magnetic field become strong.

In the case with a nonvanishing magnetic field, since we have AC and Hall conductivities, we can define a complex conductivity studied in (3.10). In figure 6, we plot such

JHEP10(2017)064

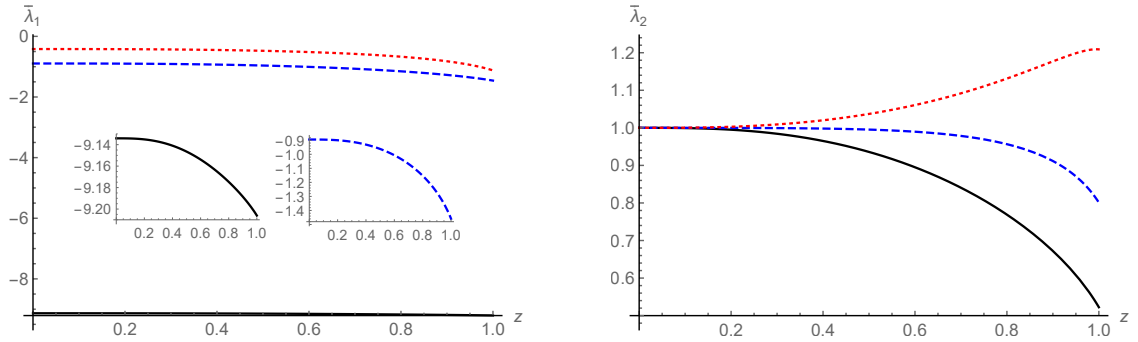

Figure 4. $\bar{\lambda}_1(z)$ and $\bar{\lambda}_2(z)$ for different values of $\bar{Q}_m = 0.1$ (black-solid) , $\sqrt{2}/2$ (blue-dashed) , 0.9 (red-dotted) where we take $k_1 = 0.1$, $k_2 = 0.4$, and $\bar{Q}_e = 0.1$.

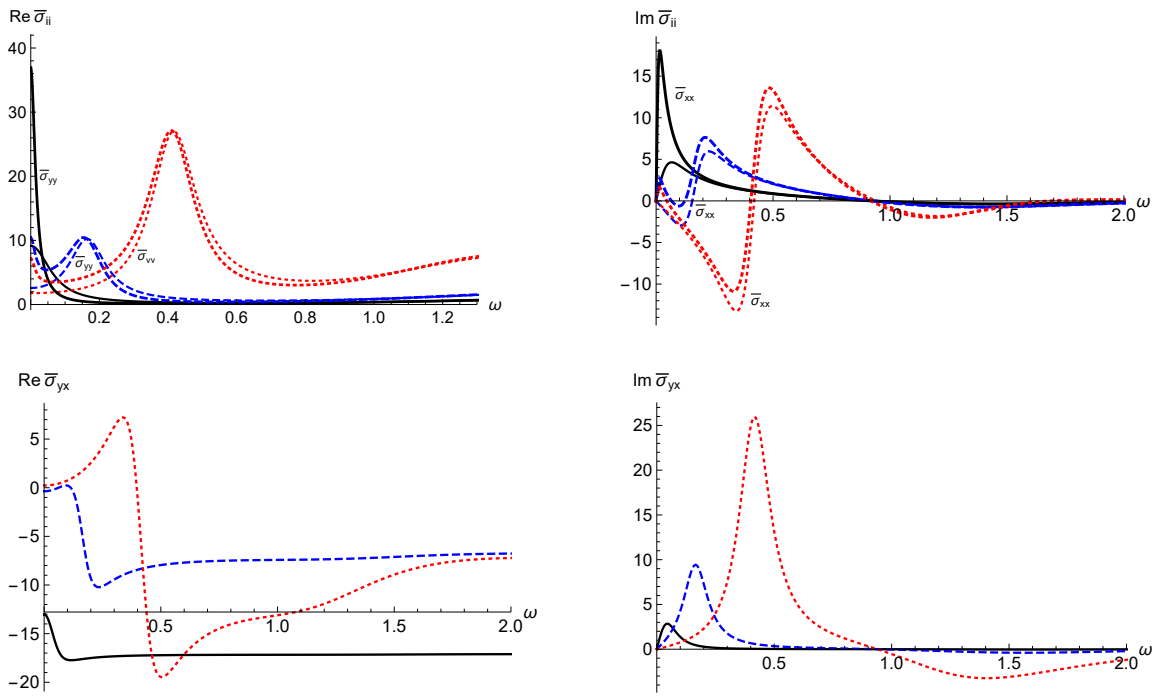

Figure 5. The AC conductivities $\bar{\sigma}_{ii}$ and Hall conductivities $\bar{\sigma}_{yx}$ in terms of frequency ω, for different values of $\bar{Q}_m = 0.1$ (black-solid) , $\sqrt{2}/2$ (blue-dashed) , 0.9 (red-dotted) where we take $k_1 = 0.1$, $k_2 = 0.4$, and $\bar{Q}_e = 0.1$. In the first two plots, we only indicate either $\bar{\sigma}_{xx}$ or $\bar{\sigma}_{yy}$, the accompanying lines are just theirs partners for $\bar{\sigma}_{yy}$ or $\bar{\sigma}_{xx}$.

a complex conductivity depending on the frequency. As expected, the peak of the complex conductivity is also shifted to the higher frequency regime as $\bar{Q}_m$ increases. The similar behaviors have also been found for the isotropic case with a nonvanishing magnetic field [13]. In the hydrodynamic limit ($\omega \ll T$) without a momentum relaxation, the complex conductivity has the following analytic form [38]

$$\tilde{g}^2\sigma_+ = i\frac{4i\tilde{Q}^2 - 4\tilde{B}\tilde{Q} + 3}{4i\tilde{B}^2 + 4\tilde{Q}\tilde{B} + 3}\,, \tag{4.18}$$

JHEP10(2017)064

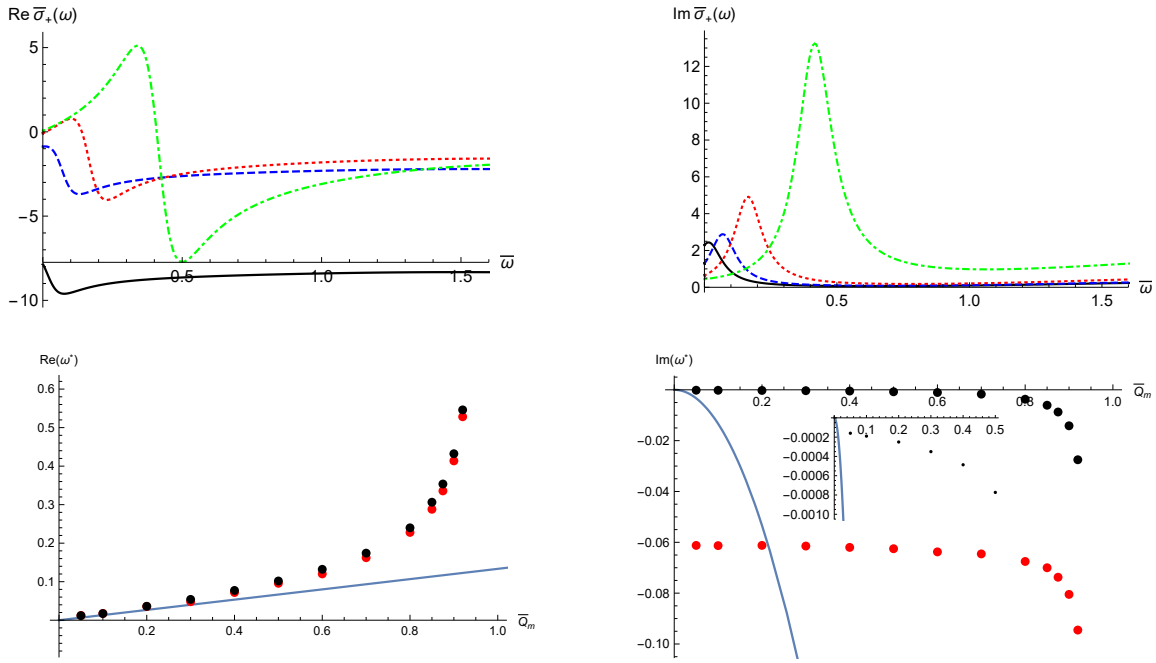

Figure 6. The plots in first row show the AC conductivities $\bar{\sigma}_+$ in terms of $\bar{\omega}$ for fixed $k_1 = 0.1$, $k_2 = 0.4$, and $\bar{Q}_e = 0.1$. With $\bar{Q}_m = 0.1, 0.4, \sqrt{2}/2, 0.9$ corresponding to black-solid, blue-dashed, red-dotted, and green-dotted-dashed curves, respectively. For dotted data in the last two plots, we show the trajectory of the pick ω^*, where $k_1 = k_2 = 10^{-4}$ (Black) and $k_1 = 0.1, k_2 = 0.4$ (Red). Also, the solid blue curves in Re(ω^*) and Im(ω^*) shows the limit of hydrodynamic of (4.19) for $\bar{Q}_e = 0.1$.

where $\tilde{Q}^2 \equiv \bar{Q}_e^2/\omega$, $\tilde{B}^2 \equiv \bar{Q}_m^2/\omega$ and $\tilde{g}^2$ indicates a field theoretic quantity, $\tilde{g}^{-2} = \sqrt{2}N^{3/2}/6\pi$. This complex conductivity allows a cyclotron frequency resonance at

$$\omega^* = -\frac{4}{3}\bar{Q}_m\left(-|\bar{Q}_e| + i\bar{Q}_m\right) . \tag{4.19}$$

Note that this formula is only valid in the hydrodynamic limit without a momentum relaxation. Interestingly, the numerical result we found in figure 6 shows a similar cyclotron frequency pole even beyond the hydrodynamic limit with a nontrivial momentum relaxation. In figure 6, the hydrodynamic limit corresponds to a small $\bar{Q}_m$ because in this case $\omega^* \ll T$. In the last two figures of figure 6, we find that the real part of cyclotron frequency pole we found numerically is well matched to the analytic result in (4.19), while imaginary part is modified by momentum relaxation [13]. Furthermore, our result shows that the cyclotron frequency pole is still alive beyond the hydrodynamic limit but cannot be explained by the hydrodynamic formula in (4.19).

In figure 7, we plot the complex conductivities of two special limits, large electric charge with $\{\bar{Q}_e, \bar{Q}_m\} = \{\sqrt{0.9}, \sqrt{0.1}\}$ and large magnetic charge with $\{\bar{Q}_e, \bar{Q}_m\} = \{\sqrt{0.1}, \sqrt{0.9}\}$. For the electric case, the pole appears at $\omega^* = 0$ as shown by the hydrodynamic formula in (4.19), whereas for the magnetic case which goes beyond the hydrodynamic limit, the cyclotron frequency pole appears in the finite frequency regime. The right hand side plot

JHEP10(2017)064

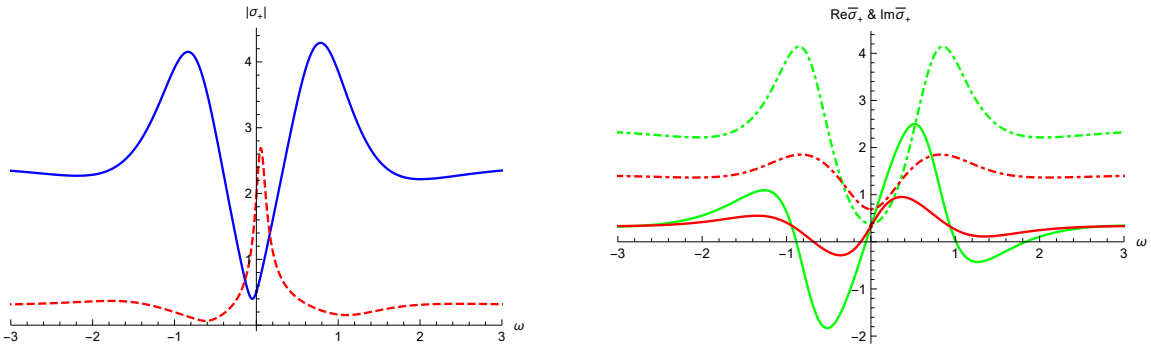

Figure 7. Left plot: the AC conductivities $|\sigma_+|$ in terms of ω, with $\bar{Q}_e = \sqrt{0.9}, \bar{Q}_m = \sqrt{0.1}$ (red-dashed curve), $\bar{Q}_e = \sqrt{0.1}, \bar{Q}_m = \sqrt{0.9}$ (Blue-solid curve). Right plot: the AC conductivities $\mathrm{Re}\bar{\sigma}_+$ (Solid curves) and $\mathrm{Im}\bar{\sigma}_+$ (Dotted-dashed curves) in terms of ω, for fixed $k_1 = 0.1$, $k_2 = 0.4$ (Green) and $k_2 = 1$ (Red), with $\bar{Q}_m = \sqrt{0.9}$ and $\bar{Q}_e = \sqrt{0.1}$.

of figure 7 shows that as the anisotropy increases (or k_2 increases) the amplitude of the cyclotron frequency pole becomes smaller. This implies that, if the system has a sufficiently large anisotropy, the cyclotron frequency pole cannot appear.

5 Conclusion

We have studied a massive gravity theory with scalar and vector fields which transform under the $\mathrm{SL}(2, R)$ group. In this case, the graviton mass breaks the diffeomorphism and generates a new physical degree of freedom represented as the Stüekelberg field. If the Stüekelberg field is given by a constant, the massive gravity is equivalent to the momentum relaxation model described by scalar fields with linear profiles. Furthermore, if we take the Stüekelberg field having different values in different spatial directions, the massive gravity we considered shows anisotropy due to the breaking of the rotational symmetry. In this work, we have investigated transport coefficients of the field theory which is dual to the anisotropic massive gravity including $\mathrm{SL}(2, R)$ transformation.

Intriguingly, we found that the equations of motion of the massive gravity are invariant under the $\mathrm{SL}(2, R)$ transformation. This fact leads to useful and important features in studying the transport coefficient because a more general solution can be easily found by applying the $\mathrm{SL}(2, R)$ transformation without solving the complicated equations of motion. After studying how a general solution can be generated from a simple solution through the $\mathrm{SL}(2, R)$ transformation, we also investigated how the physical quantity like the DC conductivity transforms under the same $\mathrm{SL}(2, R)$ transformation. We found interestingly that the complex conductivity transforms covariantly. Using this fact, one can easily calculate the DC and Hall conductivities of a general and complicated case. In addition, we also showed that the ratio of DC conductivities in different spatial directions is equal to the square of anisotropy.

We further investigate AC and Hall conductivities relying on the frequency by using the Kubo formula. After showing that the Kubo formula leads to the same DC conductivity obtained by the membrane paradigm, we studied the AC conductivity whose information

JHEP10(2017)064

cannot be obtained from the membrane paradigm. We found that the AC conductivity has a Drude-like peak when anisotropy is small. For a system having a large anisotropy, however, such a Drude-like peak disappears. When we take into account the case with a nonvanishing magnetic field, the system has an AC conductivity as well as a Hall conductivity. Similar to the membrane paradigm, we can also define a complex conductivity as the combination of AC and Hall conductivities. In the hydrodynamic limit without a momentum relaxation, it has been known that the complex conductivity has a cyclotron frequency pole. In this work, we showed that such a cyclotron frequency pole is still alive beyond the hydrodynamic limit even with an anisotropic momentum relaxation. We showed that the cyclotron frequency pole moves to the high frequency regime when the applied magnetic field becomes strong. Furthermore, we also showed that the cyclotron frequency pole cannot occur when anisotropy is sufficiently large. It would be quite interesting to find such a cyclotron resonance in real experiments.

Acknowledgments

S. Khimphun acknowledges the Korea Ministry of Science, ICT and Future Planning for the support of the Visitors Program at the Asia Pacific Center for Theoretical Physics (APCTP). This work was supported by the Korea Ministry of Education, Science and Technology, Gyeongsangbuk-Do and Pohang City. S. Khimphun and B.-H. Lee was supported by the National Research Foundation of Korea (NRF) grant funded by the Korea government MSIP No.2014R1A2A1A01002306(ERND), NRF-2017R1D1A1B03028310 and by Sogang University Research Grant (201619067.01). C. Park was also supported by Basic Science Research Program through the National Research Foundation of Korea funded by the Ministry of Education (NRF-2016R1D1A1B03932371).

References

[1] J.M. Maldacena, *The Large-N limit of superconformal field theories and supergravity*, *Int. J. Theor. Phys.* **38** (1999) 1113 [*Adv. Theor. Math. Phys.* **2** (1998) 231] [hep-th/9711200] [INSPIRE].

[2] E. Witten, *Anti-de Sitter space and holography*, *Adv. Theor. Math. Phys.* **2** (1998) 253 [hep-th/9802150] [INSPIRE].

[3] E. Witten, *Anti-de Sitter space, thermal phase transition and confinement in gauge theories*, *Adv. Theor. Math. Phys.* **2** (1998) 505 [hep-th/9803131] [INSPIRE].

[4] S.S. Gubser, I.R. Klebanov and A.M. Polyakov, *Gauge theory correlators from noncritical string theory*, *Phys. Lett.* **B 428** (1998) 105 [hep-th/9802109] [INSPIRE].

[5] G. Policastro, D.T. Son and A.O. Starinets, *From AdS/CFT correspondence to hydrodynamics*, *JHEP* **09** (2002) 043 [hep-th/0205052] [INSPIRE].

JHEP10(2017)064

[6] G. Policastro, D.T. Son and A.O. Starinets, *From AdS/CFT correspondence to hydrodynamics. 2. Sound waves*, *JHEP* **12** (2002) 054 [hep-th/0210220] [INSPIRE].

[7] C.P. Herzog, P. Kovtun, S. Sachdev and D.T. Son, *Quantum critical transport, duality and M-theory*, *Phys. Rev.* **D 75** (2007) 085020 [hep-th/0701036] [INSPIRE].

[8] G.T. Horowitz, J.E. Santos and D. Tong, *Optical Conductivity with Holographic Lattices*, *JHEP* **07** (2012) 168 [arXiv:1204.0519] [INSPIRE].

[9] G.T. Horowitz, J.E. Santos and D. Tong, *Further Evidence for Lattice-Induced Scaling*, *JHEP* **11** (2012) 102 [arXiv:1209.1098] [INSPIRE].

[10] M. Taylor, *Non-relativistic holography*, arXiv:0812.0530 [INSPIRE].

[11] T. Andrade and B. Withers, *A simple holographic model of momentum relaxation*, *JHEP* **05** (2014) 101 [arXiv:1311.5157].

[12] M. Blake and A. Donos, *Quantum Critical Transport and the Hall Angle*, *Phys. Rev. Lett.* **114** (2015) 021601 [arXiv:1406.1659] [INSPIRE].

[13] K.-Y. Kim, K.K. Kim, Y. Seo and S.-J. Sin, *Thermoelectric Conductivities at Finite Magnetic Field and the Nernst Effect*, *JHEP* **07** (2015) 027 [arXiv:1502.05386] [INSPIRE].

[14] P. Chesler, A. Lucas and S. Sachdev, *Conformal field theories in a periodic potential: results from holography and field theory*, *Phys. Rev.* **D 89** (2014) 026005 [arXiv:1308.0329] [INSPIRE].

[15] Y. Ling, C. Niu, J.-P. Wu and Z.-Y. Xian, *Holographic Lattice in Einstein-Maxwell-Dilaton Gravity*, *JHEP* **11** (2013) 006 [arXiv:1309.4580] [INSPIRE].

[16] A. Donos and J.P. Gauntlett, *Thermoelectric DC conductivities from black hole horizons*, *JHEP* **11** (2014) 081 [arXiv:1406.4742] [INSPIRE].

[17] A. Donos and J.P. Gauntlett, *The thermoelectric properties of inhomogeneous holographic lattices*, *JHEP* **01** (2015) 035 [arXiv:1409.6875] [INSPIRE].

[18] D. Vegh, *Holography without translational symmetry*, arXiv:1301.0537 [INSPIRE].

[19] R.A. Davison, *Momentum relaxation in holographic massive gravity*, *Phys. Rev.* **D 88** (2013) 086003 [arXiv:1306.5792] [INSPIRE].

[20] M. Blake and D. Tong, *Universal Resistivity from Holographic Massive Gravity*, *Phys. Rev.* **D 88** (2013) 106004 [arXiv:1308.4970] [INSPIRE].

[21] L. Alberte and A. Khmelnitsky, *Stability of Massive Gravity Solutions for Holographic Conductivity*, *Phys. Rev.* **D 91** (2015) 046006 [arXiv:1411.3027] [INSPIRE].

[22] Z. Zhou, J.-P. Wu and Y. Ling, *DC and Hall conductivity in holographic massive Einstein-Maxwell-Dilaton gravity*, *JHEP* **08** (2015) 067 [arXiv:1504.00535] [INSPIRE].

[23] L. Alberte, M. Baggioli, A. Khmelnitsky and O. Pujolàs, *Solid Holography and Massive Gravity*, *JHEP* **02** (2016) 114 [arXiv:1510.09089] [INSPIRE].

[24] A. Sen, *Electric magnetic duality in string theory*, *Nucl. Phys.* **B 404** (1993) 109 [hep-th/9207053] [INSPIRE].

[25] K. Goldstein, N. Iizuka, R.P. Jena and S.P. Trivedi, *Non-supersymmetric attractors*, *Phys. Rev.* **D 72** (2005) 124021 [hep-th/0507096] [INSPIRE].

[26] N. Iizuka, *Non-supersymmetric attractors*, *Nucl. Phys. Proc. Suppl.* **171** (2007) 286 [INSPIRE].

JHEP10(2017)064

[27] K. Goldstein, S. Kachru, S. Prakash and S.P. Trivedi, *Holography of Charged Dilaton Black Holes*, *JHEP* **08** (2010) 078 [arXiv:0911.3586] [INSPIRE].

[28] K. Goldstein, N. Iizuka, S. Kachru, S. Prakash, S.P. Trivedi and A. Westphal, *Holography of Dyonic Dilaton Black Branes*, *JHEP* **10** (2010) 027 [arXiv:1007.2490] [INSPIRE].

[29] A. Bayntun, C.P. Burgess, B.P. Dolan and S.-S. Lee, *AdS/QHE: Towards a Holographic Description of Quantum Hall Experiments*, *New J. Phys.* **13** (2011) 035012 [arXiv:1008.1917] [INSPIRE].

[30] N. Iizuka and K. Maeda, *Study of Anisotropic Black Branes in Asymptotically anti-de Sitter*, *JHEP* **07** (2012) 129 [arXiv:1204.3008] [INSPIRE].

[31] X.-H. Ge, Y. Ling, C. Niu and S.-J. Sin, *Thermoelectric conductivities, shear viscosity and stability in an anisotropic linear axion model*, *Phys. Rev.* **D 92** (2015) 106005 [arXiv:1412.8346] [INSPIRE].

[32] S. Jain, R. Samanta and S.P. Trivedi, *The Shear Viscosity in Anisotropic Phases*, *JHEP* **10** (2015) 028 [arXiv:1506.01899] [INSPIRE].

[33] S. Jain, N. Kundu, K. Sen, A. Sinha and S.P. Trivedi, *A Strongly Coupled Anisotropic Fluid From Dilaton Driven Holography*, *JHEP* **01** (2015) 005 [arXiv:1406.4874] [INSPIRE].

[34] D. Roychowdhury, *On anisotropic black branes with Lifshitz scaling*, *Phys. Lett.* **B 759** (2016) 410 [arXiv:1509.05229] [INSPIRE].

[35] D. Roychowdhury, *Holography for anisotropic branes with hyperscaling violation*, *JHEP* **01** (2016) 105 [arXiv:1511.06842] [INSPIRE].

[36] S. Khimphun, B.-H. Lee and C. Park, *Conductivities in an anisotropic medium*, *Phys. Rev.* **D 94** (2016) 086005 [arXiv:1604.00156] [INSPIRE].

[37] S.A. Hartnoll, P.K. Kovtun, M. Muller and S. Sachdev, *Theory of the Nernst effect near quantum phase transitions in condensed matter and in dyonic black holes*, *Phys. Rev.* **B 76** (2007) 144502 [arXiv:0706.3215] [INSPIRE].

[38] S.A. Hartnoll and C.P. Herzog, *Ohm's Law at strong coupling: S duality and the cyclotron resonance*, *Phys. Rev.* **D 76** (2007) 106012 [arXiv:0706.3228] [INSPIRE].

[39] C. de Rham, G. Gabadadze and A.J. Tolley, *Resummation of Massive Gravity*, *Phys. Rev. Lett.* **106** (2011) 231101 [arXiv:1011.1232] [INSPIRE].

[40] K. Hinterbichler, *Theoretical Aspects of Massive Gravity*, *Rev. Mod. Phys.* **84** (2012) 671 [arXiv:1105.3735] [INSPIRE].

[41] R.-G. Cai, Y.-P. Hu, Q.-Y. Pan and Y.-L. Zhang, *Thermodynamics of Black Holes in Massive Gravity*, *Phys. Rev.* **D 91** (2015) 024032 [arXiv:1409.2369] [INSPIRE].

[42] L.-M. Cao, Y. Peng and Y.-L. Zhang, *de Rham-Gabadadze-Tolley massive gravity with degenerate reference metrics*, *Phys. Rev.* **D 93** (2016) 124015 [arXiv:1511.04967] [INSPIRE].

[43] A.D. Shapere, S. Trivedi and F. Wilczek, *Dual dilaton dyons*, *Mod. Phys. Lett.* **A 6** (1991) 2677 [INSPIRE].

[44] M. Parikh and F. Wilczek, *An Action for black hole membranes*, *Phys. Rev.* **D 58** (1998) 064011 [gr-qc/9712077] [INSPIRE].

[45] N. Iqbal and H. Liu, *Universality of the hydrodynamic limit in AdS/CFT and the membrane paradigm*, *Phys. Rev.* **D 79** (2009) 025023 [arXiv:0809.3808] [INSPIRE].

JHEP10(2017)064

[46] J. de Boer, E.P. Verlinde and H.L. Verlinde, *On the holographic renormalization group*, *JHEP* **08** (2000) 003 [hep-th/9912012] [INSPIRE].

[47] V. Balasubramanian and P. Kraus, *A Stress tensor for Anti-de Sitter gravity*, *Commun. Math. Phys.* **208** (1999) 413 [hep-th/9902121] [INSPIRE].

[48] S. de Haro, S.N. Solodukhin and K. Skenderis, *Holographic reconstruction of space-time and renormalization in the AdS/CFT correspondence*, *Commun. Math. Phys.* **217** (2001) 595 [hep-th/0002230] [INSPIRE].

[49] C. Park, *Holographic Aspects of a Relativistic Nonconformal Theory*, *Adv. High Energy Phys.* **2013** (2013) 389541 [arXiv:1209.0842] [INSPIRE].

[50] C. Park, *Massive quasinormal mode in the holographic Lifshitz Theory*, *Phys. Rev.* **D 89** (2014) 066003 [arXiv:1312.0826] [INSPIRE].

[51] C. Park, *Holographic renormalization in dense medium*, *Adv. High Energy Phys.* **2014** (2014) 565219 [arXiv:1405.1490] [INSPIRE].

[52] A. Amoretti and D. Musso, *Magneto-transport from momentum dissipating holography*, *JHEP* **09** (2015) 094 [arXiv:1502.02631] [INSPIRE].

[53] M. Blake, *Magnetotransport from the fluid/gravity correspondence*, *JHEP* **10** (2015) 078 [arXiv:1507.04870] [INSPIRE].

[54] A. Amoretti, M. Baggioli, N. Magnoli and D. Musso, *Chasing the cuprates with dilatonic dyons*, *JHEP* **06** (2016) 113 [arXiv:1603.03029] [INSPIRE].

[55] A. Donos, J.P. Gauntlett, T. Griffin, N. Lohitsiri and L. Melgar, *Holographic DC conductivity and Onsager relations*, *JHEP* **07** (2017) 006 [arXiv:1704.05141] [INSPIRE].

[56] X.-H. Ge, Y. Tian, S.-Y. Wu and S.-F. Wu, *Hyperscaling violating black hole solutions and Magneto-thermoelectric DC conductivities in holography*, *Phys. Rev.* **D 96** (2017) 046015 [arXiv:1606.05959] [INSPIRE].

[57] J.-i. Koga, K. Maeda and K. Tomoda, *Holographic superconductor model in a spatially anisotropic background*, *Phys. Rev.* **D 89** (2014) 104024 [arXiv:1401.6501] [INSPIRE].

[58] M. Baggioli and O. Pujolàs, *Electron-Phonon Interactions, Metal-Insulator Transitions and Holographic Massive Gravity*, *Phys. Rev. Lett.* **114** (2015) 251602 [arXiv:1411.1003] [INSPIRE].

[59] M. Baggioli and O. Pujolàs, *On Effective Holographic Mott Insulators*, *JHEP* **12** (2016) 107 [arXiv:1604.08915] [INSPIRE].

[60] M. Baggioli and M. Goykhman, *Phases of holographic superconductors with broken translational symmetry*, *JHEP* **07** (2015) 035 [arXiv:1504.05561] [INSPIRE].

[61] D.V.d. Marel et al., *Powerlaw optical conductivity with a constant phase angle in high Tc superconductors*, *Nature* **425** (2003) 271 [cond-mat/0309172].

JHEP10(2017)064